archives
of thermodynamics
Vol. **40**(2019), No. 3, 137–157
DOI: 10.24425/ather.2019.129998

Comparison of an impulse and a reaction turbine stage for an ORC power plant

DAWID ZANIEWSKI*
PIOTR KLIMASZEWSKI
ŁUKASZ WITANOWSKI
ŁUKASZ JĘDRZEJEWSKI
PIOTR KLONOWICZ
PIOTR LAMPART

Institute of Fluid Flow Machinery Polish Academy of Sciences, Centre of Heat and Power Engineering, Turbine Department, Fiszera 14, 80-231 Gdańsk, Poland

Abstract Turbine stages can be divided into two types: impulse stages and reaction stages. The advantages of one type over the second one are generally known based on the basic physics of turbine stage. In this paper these differences between mentioned two types of turbines were indicated on the example of single stage turbines dedicated to work in organic Rankine cycle (ORC) power systems. The turbines for two ORC cases were analysed: the plant generating up to 30 kW and up to 300 kW of net electric power, respectively. Mentioned ORC systems operate with different working fluids: DMC (dimethyl carbonate) for the 30 kW power plant and MM (hexamethyldisiloxane) for the 300 kW power plant. The turbines were compared according to three major issues: thermodynamic and aerodynamic performance, mechanical and manufacturing aspects. The analysis was performed by means of the 0D turbomachinery theory and 3D computational aerodynamic calculations. As a result of this analysis, the paper indicates conclusions which type of turbine is a recommended choice to use in ORC systems taking into account the features of these systems.

Keywords: CFD; Waste heat recovery; Steam turbine; Organic Rankine cycle

*Corresponding Author. Email: dzaniewski@imp.gda.pl

Nomenclature

b	–	chord of a profile, mm
c	–	velocity in the stationary frame, m/s
c_s	–	spouting velocity, m/s
D/l	–	mean diameter related to the height of a blade
l	–	height of a blade, mm
L_{ax}	–	axial length of a blade, mm
M	–	Mach number
P_{NET}	–	net power produced by a turbine obtained making use of 0D theory, kW
R	–	mean radius of a stator/rotor, mm
R_h	–	hub radius of a stator/rotor, mm
R_s	–	external radius of a stator/rotor, mm
u	–	peripheral speed, m/s
w	–	velocity in the rotating frame, m/s
Z	–	quantity of blades of a rotor/stator

Greek symbols

α	–	angle of the stream in the stationary frame, $^\circ$
β	–	angle of the stream in the rotating frame, $^\circ$
η_{ETN}	–	net isentropic efficiency obtained making use of 0D theory,%
$\eta_{\text{NET\_CFD}}$	–	net isentropic efficiency calculated making use of CFD, %
Θ_h	–	degree of reaction at the hub, %
$\triangle h$	–	energy losses, kJ/kg

1 Introduction

In general turbines can be divided into two types: the impulse type which has the degree of reaction equal to 0 and the reaction type with the degree of reaction equal to 0.5. The degree of reaction can be described as a ratio of the isentropic enthalpy drop in a rotor to the isentropic enthalpy drop in the whole stage. This distinction has a historical meaning because presently turbines are usually designed with a degree of reaction between 0 and 0.5 or sometimes even more than 0.5. The conventional distinction determines the impulse turbines as machines with the degree of reaction between 0 and 0.3 and the reaction turbines as machines with the degree of reaction greater than 0.3 up to 0.5 (or more) but anyway this distinction has a smooth boundary [1–3]. Because of a few principal differences, these two types of machines have a different construction. It applies especially to axial turbines. Radial turbines (radial inflow and radial outflow) are usually designed as a reaction type [4–6] although there are designs with a low degree of reaction [7–10].

Each type of turbine has specific advantages and disadvantages. In general the comparison of these two types of machines should include the following points:

- thermodynamic and aerodynamic performance,
- parameters of work which affect the construction of a machine,
- technological challenge during manufacturing of parts of the machines.

A few advantages of one type over the second one are generally known and based on the fundamental physics of turbines. These examples are described below.

The impulse turbine accelerates gas mainly during expansion in nozzles. Because of that the absolute outlet velocity from the vane is much higher than in the reaction turbine. It leads to greater losses during flow through the channel. Thus the impulse turbine efficiency potential is generally lower than that of the reaction turbine [1–3,11]. Because of expansion in the rotor of the reaction turbine there is a pressure difference between the rotor inlet and outlet. It leads to higher tip clearance losses for the reaction turbine than for the impulse one in case of an identical tip clearance [11]. The mentioned pressure difference causes also the axial thrust which has to be countered by the thrust bearing and sometimes has to be balanced using the high pressure gas in the form of a so called relief piston [1,2,11]. Another advantage of the impulse turbine over the reaction one is much lower optimal peripheral speed, which is significantly lower for the identical enthalpy drop. It leads to lower stress in rotating parts during the turbine operation [3,4,11].

The paper presents analysis of two types of turbines: the axial impulse type and the radial inflow reaction type. An analysis was done for turbines dedicated to work in organic Rankine cycle (ORC). The first case considers an ORC system generating about 30 kW of electrical power which is working with DMC (dimethyl carbonate) fluid. The second case considers a power plant generating about 300 kW of electrical power and working with MM (hexamethyldisiloxane) fluid.

The design calculations of mentioned turbines were performed by means of 0D theory (zero dimensional preliminary stage flow calculations) [1,2] and detailed analysis was done through computational fluid dynamics [12] using commercial engineering simulation software Ansys CFX [13]. The purpose of the analysis is to compare the radial and the axial turbine for the specific application mentioned above.

2 Turbine stage calculations

2.1 Boundary conditions

The boundary conditions for the 0D and the 3D fluid flow analysis were obtained from the ORC heat balance calculation. The following parameters were used: inlet total pressure, inlet total temperature, outlet static pressure and nominal rotational speed. For 0D analysis the value of mass flow rate was also included. The analysed cases were ordered as follows:

- Case 1. The ORC plant with the DMC as working fluid – net power equal to about 30 kWel:
  - ▷ A – axial impulse turbine with a low degree of reaction,
  - ▷ B – axial impulse turbine with a considerable degree of reaction,
  - ▷ C – radial inflow reaction turbine.
- Case 2. The ORC plant with the MM fluid – net nominal power up to 300 kWel:
  - ▷ A – axial impulse turbine with a considerable degree of reaction,
  - ▷ B – radial inflow reaction turbine.

The values of the boundary parameters for all cases are shown in Tab. 1.

Table 1: Values of the boundary parameters of the all analysed cases.

Parameters	Case 1.			Case 2.	
Boundary parameters	A	B	C	A	B
Degree of reaction in the mean radius [%]	9.3	25.2	49.5	27.6	50.0
Opt. rotational speed of rotor [rpm]	40000	41000	51555	14500	11000
Inlet total pressure [kPa] (abs)	1500			1026	
Inlet total temperature [°C]	211.2			210.47	
Outlet static pressure [kPa] (abs)	23			21	
Mass flow rate [kg/s]	0.396			5.759	
Isentropic enthalpy drop [kJ/kg]	152.6			82.52	

2.2 0D turbine theory

The 0D theory of turbomachinery which was used is the well-known method of preliminary design of turbine stages. It allows a designer to shape the initial geometry of the blades and the channel. This theory is usually enriched by additional empirical correlations for different kind of losses which could occur during flow through the channel so that the calculation results become more realistic [14]. Basically the 0D theory is based on Euler's turbomachinery equation, the continuity equation and the law of conservation of energy [1–3]. Additionally, loss correlations were used [15].

The profiles shape was generated making use of the in-house software which is based on the 0D theory results and the commercial software Ansys BladeGen [16].

2.3 CFD analysis setup

The computational fluid dynamics (CFD) analysis was performed as a steady state with the multiply frame of reference interface ('frozen rotor') between the stator and rotor domains. The shroud, hub and blade surfaces were defined as non-slip adiabatic smooth walls. The periodic boundary were used as single blade channels were modelled. The tip clearance was not included in the analysis. The turbulence model used in the analysis was k-ω shear stress transport (SST).

3 Results of the analysis and conclusions

3.1 Case 1 – up to 30 kW ORC plant with DMC fluid

In the first step the axial impulse turbine with a low degree of reaction (Tabs. 2, 5, 6, and Figs. 1, 4, 5) and with a higher degree of reaction (Tabs. 3, 7, 8, and Figs. 2, 6, 7) are compared for the first case: A and B. For Case 1A the degree of reaction in the mean radius is 9.3% and this leads to the negative degree of reaction at the hub. Situation like this usually causes the separation of the fluid at the hub which leads to additional loss. The turbine from Case 1B has the mean degree of reaction equal to 25.2%. This value is big enough to receive the positive value of this parameter at the hub.

As it was mentioned before the impulse turbine will achieve a much higher outlet velocity from the nozzle (Figs. 4 and 6) for the same total enthalpy drop. For Case 1A the value of this parameter is by 16% greater than it is for Case 1B. This fact and the mentioned problems with a negative degree of reaction at the rotor hub yield lower isentropic efficiency (total to static) of the impulse turbine – 3.2 percent points lower than it is for the other turbine.

In Case 1C (the radial inflow reaction turbine) all the calculations results are presented in Tabs. 4, 9, 10 and Figs. 3, 8, 9. In this case with the mean degree of reaction equal to 50% the outlet velocity from the nozzle is almost 30% lower than that in Case 1A – impulse axial turbine (Figs. 4 and 8). It is one of the major reasons that the isentropic efficiency of this turbine achieves 85.3% (Tab. 10) which is 8.5 percent point more than for the impulse turbine with a low degree of reaction and 5.3 percent point more than for the other impulse turbine with a considerable degree of reaction. The impulse turbine has the lower isentropic efficiency also because of a relatively higher flow turning angle in the rotor channel which is the reason of additional profile loss and endwall loss. Another reason for the high isentropic efficiency of the radial reaction turbine is the attribute of the radial stage which is more efficient than axial impulse stage according to Euler's equation. It is the reason why the axial impulse stage and the radial reaction stage could not easily be compared.

Case 1A and 1B have almost equal optimal rotational velocities (40 000 and 41 000 rpm, respectively, Tab. 1). Case 1B has a higher value of peripheral speed which yields greater dimensions of turbine wheels (Tab. 2, Fig. 1 and Tab. 3, Fig. 2) for the optimal design velocity ratio. A direct consequence of that is greater design challenge from the mechanical point of view.

The optimal rotational speed of the turbine in Case 1C is higher than that in Cases 1A and 1B (Tab. 1). It leads to more problems with rotordynamic and structural aspects of the machine. The diameter of the rotor in the nozzle outlet control section is similar to that from case 1B (Tab. 3, Fig. 2 and Tab. 4, Fig. 3). It means that in conjunction with a greater rotational speed this type of turbine will feature a higher peripheral speed. The 50% degree of reaction leads also to a relatively high pressure drop during flow through the rotor, so for the similar diameters of rotors from Case 1B and Case 1C the second one will receive much more axial thrust. All of these aspects are the reasons why the radial inflow reaction turbine is more difficult to design, also because of much more demanding shape of the rotor which is more difficult to manufacture.

Table 2: The axial impulse turbine (with a low degree of reaction) main dimensions – Case 1A (DMC fluid, 30 kW plant.

Control section	R [mm]	R_h [mm]	R_s [mm]	l [mm]	D/l [mm]	L_{ax} [mm]	b [mm]	Z [–]
Nozzle (inlet)	57.7	53.1	62	8.9	–	–	–	–
Nozzle (outlet)	57.7	53.1	62	8.9	13	30	60	16/16
Rotor (outlet)	59.2	52.8	65	12.2	9.5	13.6	13.6	41

Table 3: The axial impulse turbine (with a considerable degree of reaction) main dimensions – Case 1B (DMC fluid, 30 kW plant).

Control section	R [mm]	R_h [mm]	R_s [mm]	l [mm]	D/l [mm]	L_{ax} [mm]	b [mm]	Z [–]
Nozzle (inlet)	67.7	65	70.3	5.3	–	–	–	–
Nozzle (outlet)	67.7	65	70.3	5.3	25.5	36	72	16/16
Rotor (outlet)	70.4	62.5	77.5	15	9	25	25	27

Table 4: The radial inflow reaction turbine main dimensions – Case 1C (DMC fluid, 30 kW plant).

Control section	R [mm]	R_h [mm]	R_s [mm]	l [mm]	D/l [mm]	L_{ax} [mm]	b [mm]	Z [–]
Nozzle (inlet)	91	91	91	2.7	–	–	–	–
Nozzle (outlet)	68.561	68.561	68.561	2.7	50	2.7	40	16/16
Rotor (outlet)	35.6517	16	48	32	2.22	48	80	13

In Figs. 5, 7, and 9 it is possible to observe that in all the considered cases flow is supersonic both in the stator and rotor, except for the rotor in Case 1C, where the flow is transonic. In the same figures it is possible to observe the shock structures, especially: 'fish-tail shocks' on the trailing edges and 'bow shocks' (with their reflections along the rotor channel) on

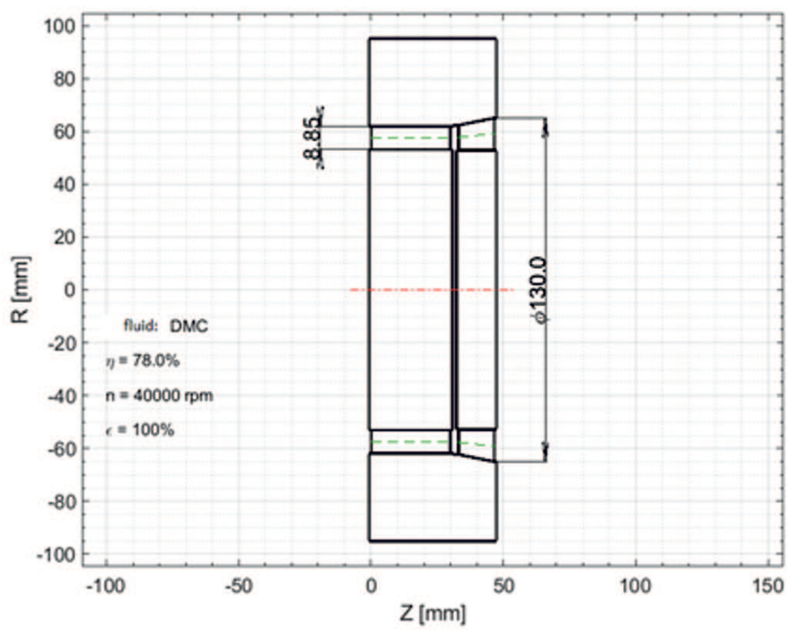

Figure 1: The axial impulse turbine (with low degree of reaction) stage sketch – Case 1A (DMC fluid, 30 kW plant).

Table 5: Kinematics values of the mean stream – Case 1A (DMC fluid, 30 kW plant).

Control section	c [m/s]	w [m/s]	u [m/s]	α [°]	β [°]	M [–]	Δh_s [kJ/kg]	u/c_s [–]
Nozzle (outlet)	499.16	271.86	241.67	14.43	27.22	2.580	13.84	0.45
Rotor I (outlet)	134.61	290.37	248.04	94.01	152.45	1.503	10.54	0.45

the leading edges of the rotor. In Case 1C it is difficult to observe any shockwaves in the rotor region. It is very important that the observed shockwaves are relatively weak, therefore they are not the major part of flow losses. It has to be kept in mind that the shockwaves structures have unsteady character and cannot be analysed properly in the case of steady state analysis.

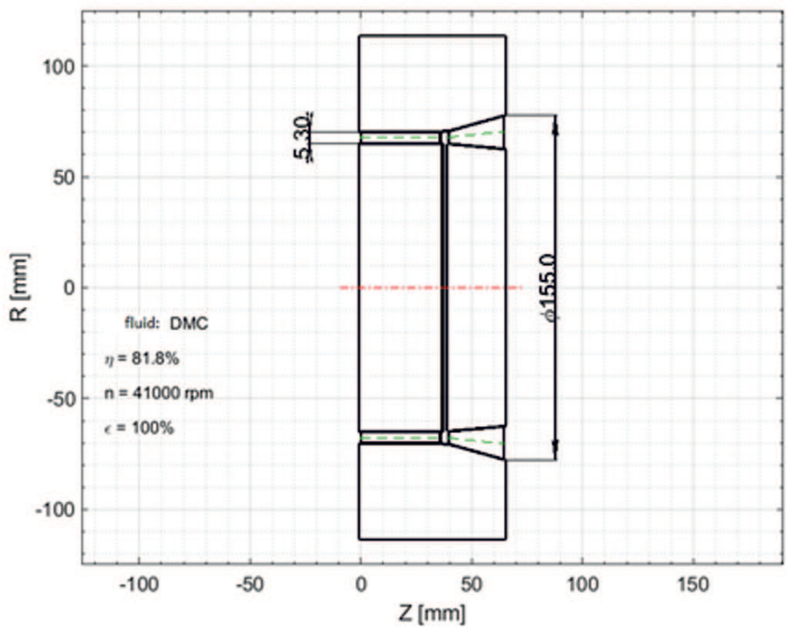

Figure 2: The axial impulse turbine (with low degree of reaction) stage sketch – Case 1A (DMC fluid, 30 kW plant).

Table 6: Performance of the axial impulse turbine (with a low degree of reaction) – Case 1A (DMC fluid, 30 kW plant).

P_{NET} [kW]	η_{NET} [%]	$\eta_{\mathrm{NET\_CFD}}$ [%]	Θ_h [%]
47.13	78.0	76.8	-6.0

Because of the fact that the tip clearance flow losses were not included in this paper the differences of efficiencies between particular axial and radial stages could be smaller. Anyway it is possible to decrease the tip clearance losses making use of different types of seals, e.g. labyrinth (if a shrouding is added), honeycomb, brush, etc.

The ORC micro turbines for small power generation are featured by relatively small mass flow rates and strongly supersonic flows. These two

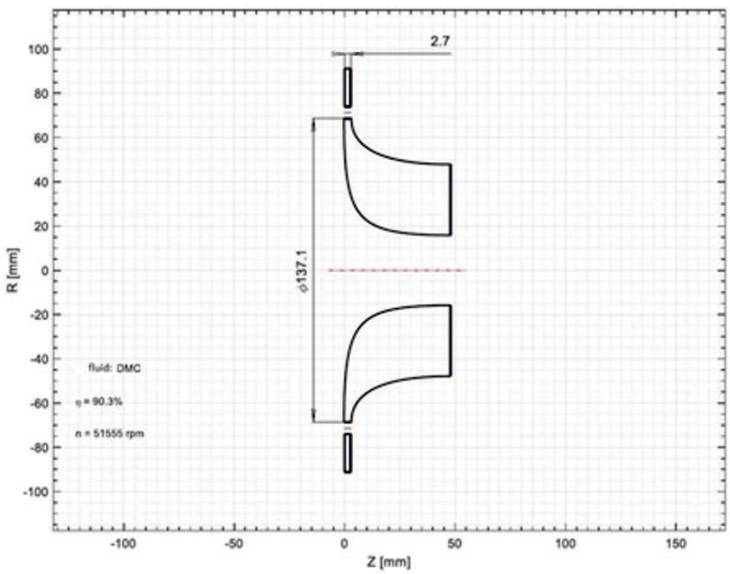

Figure 3: The radial inflow reaction turbine stage sketch – Case 1C (DMC fluid, 30 kW plant).

Table 7: Kinematics values of the mean stream – Case 1B (DMC fluid, 30 kW plant).

Control section	c [m/s]	w [m/s]	u [m/s]	α [°]	β [°]	M [–]	Δh_s [kJ/kg]	u/c_s [–]
Nozzle (outlet)	453.4	178.57	290.68	11.63	30.78	2.312	11.42	0.55
Rotor I (outlet)	92.44	304.05	302.27	82.32	162.46	1.576	11.56	0.55

Table 8: Performance of the axial impulse turbine (with considerable degree of reaction) – Case 1B (DMC fluid, 30 kW plant).

P_{NET} [kW]	η_{NET} [%]	$\eta_{\mathrm{NET\_CFD}}$ [%]	Θ_h [%]
49.43	81.8	80.0	19.0

aspects lead to the fact that a turbine nozzle has to be designed as a de Laval nozzle with very small critical section which means that the throat between the blades can be even less than 1 mm (e.g. turbines from Cases 1A,

Table 9: Kinematics values of the mean stream – Case 1C (DMC fluid, 30 kW plant).

Control section	c [m/s]	w [m/s]	u [m/s]	α [°]	β [°]	M [–]	Δh_s [kJ/kg]	u/c_s [–]
Nozzle (outlet)	376.45	65.37	370.15	10	89.49	1.90	6.10	0.67
Rotor I (outlet)	91.568	215.90	192.48	91.92	154.92	1.13	5.27	0.67

Table 10: Performance of the radial inflow reaction turbine – Case 1C (DMC fluid, 30 kW plant).

P_{NET} [kW]	η_{NET} [%]	$\eta_{\mathrm{NET\_CFD}}$ [%]
54.6	90.3	85.3

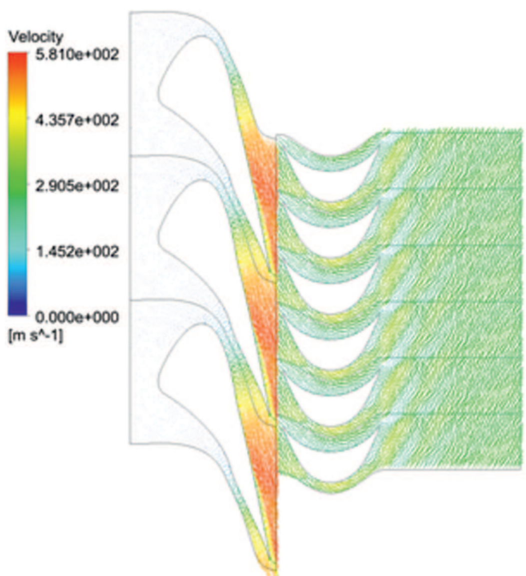

Figure 4: Velocity vectors at the mean diameter of the axial impulse turbine (with low degree of reaction) – Case 1A (DMC fluid, 30 kW plant).

1B and 1C). Such channels can be extremely difficult to manufacture (with acceptable tolerances) what is the reason why nozzles of those turbines have to be specially shaped (contoured) through the meridional section as well.

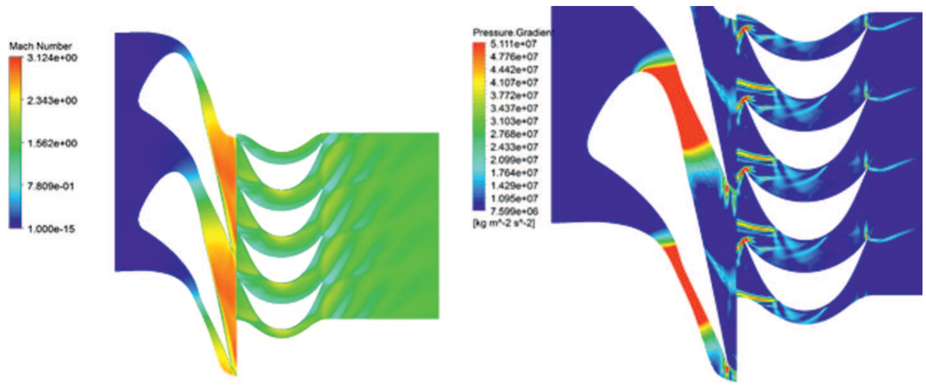

Figure 5: Mach Number contours (left side) and pressure gradient contours (right side) at the mean diameter of the axial impulse turbine (with low degree of reaction) – Case 1A (DMC fluid, 30 kW plant).

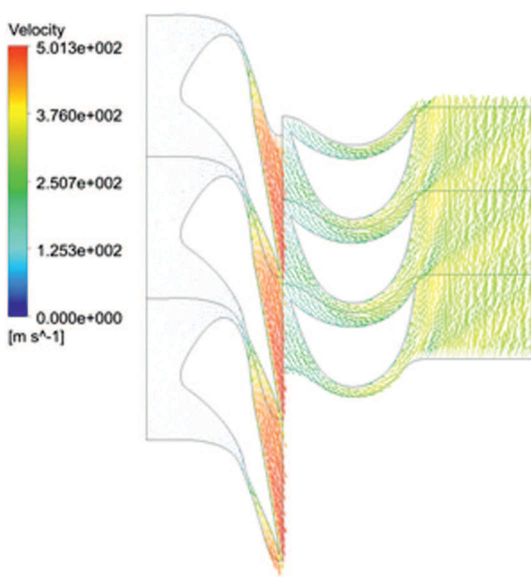

Figure 6: Velocity vectors at the mean diameter of the axial impulse turbine (with considerable degree of reaction) – Case 1B (DMC fluid, 30 kW plant).

The considered ORC turbine will be part of a hermetic micro turbogenerator characterised by a compact construction. Because of that it is very important to prepare a design which is a compromise between small

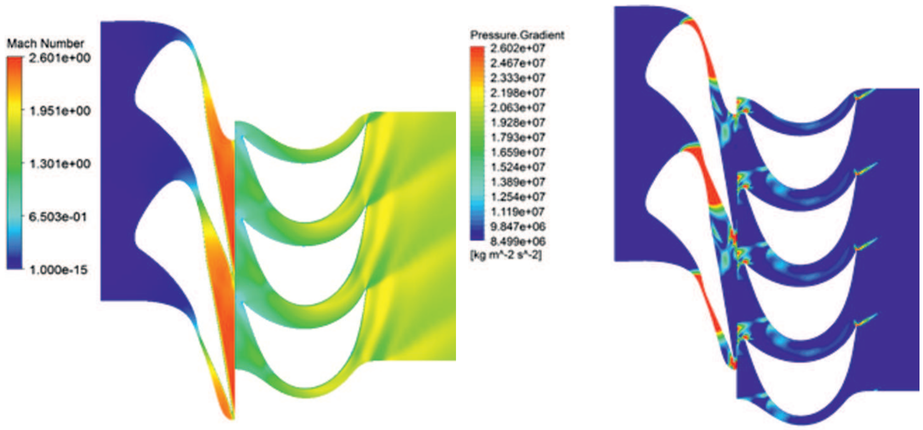

Figure 7: Mach Number contours (left side) and pressure gradient contours (right side) at the mean diameter of the axial impulse turbine (with considerable degree of reaction) – Case 1B (DMC fluid, 30 kW plant).

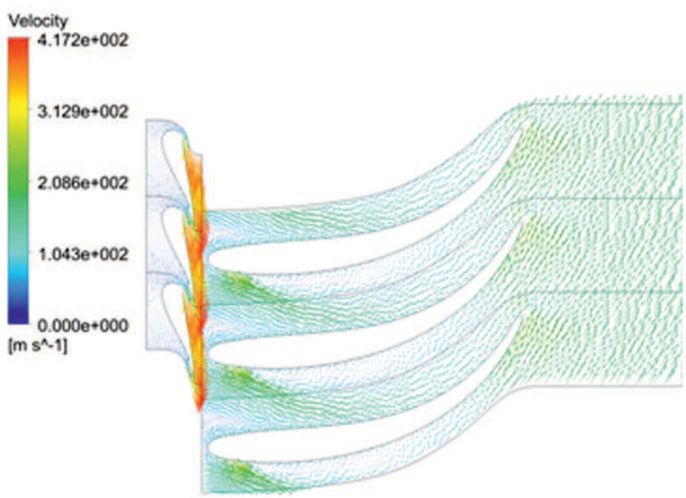

Figure 8: Velocity vectors at the mean diameter of the radial reaction turbine – Case 1C (DMC fluid, 30 kW plant).

dimensions, acceptable axial thrust, relatively high efficiency and simplicity of machining. It is clear that the impulse type stage will result in a lower value of axial thrust. As it was shown that dimensions of the impulse type stage will be smaller and much easier to manufacture. An advantage of the

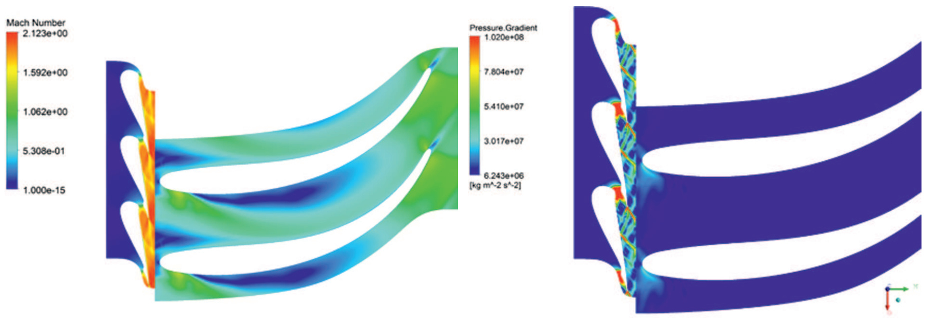

Figure 9: Mach Number contours (a top image) and pressure gradient contours (a bottom image) at the mean diameter of the radial reaction turbine – Case 1C (DMC fluid, 30 kW plant).

reaction type stage is a greater isentropic efficiency. Anyway, the calculated difference in isentropic efficiency between the reaction and impulse turbine stage is not large (especially for this relatively small amount of nominal power) and, as it was mentioned before that difference can be even smaller while the tip leakage is included in the calculations. For this reason the authors recommend Case 1B as a suitable choice for the design of small power ORC units.

3.2 Case 2 – up to 300 kWel ORC plant with MM fluid

In Case 2 all the calculations results are presented in Tabs. 11, 13, 14, and Figs. 10, 12, 13 (for Case 2A) and Tabs. 12, 15, 16, and Figs. 11, 14, 15 (for Case 2B).

During the comparison of turbines from Cases 2A and 2B (Tab. 1) it could be observed that in terms of the nozzle outlet velocity (Figs. 12 and 14) and the isentropic efficiency (Tabs. 14 and 16) the trend is similar to the turbines from Case 1. The outlet nozzle velocity in the impulse stage is by 26% greater than that in the reaction turbine. The isentropic efficiency is approximately by 8 percent point higher for the radial reaction stage.

For Case 2 (the large turbines) one can observe in Tab. 11, Fig. 10 and Tab. 12, Fig. 11 that the outer diameter of the reaction turbine rotor wheel is by 66% greater than in the case of the axial impulse turbine. It intensifies the axial thrust problem of the radial reaction turbine in comparison to the turbines from Case 1.

The optimal rotational speed is 25% smaller for the radial reaction stage (Case 2B) than in the case of axial impulse stage (Case 2A). Anyway much greater dimensions of the rotor probably will cause more problems with rotordynamic aspects of a machine.

As it was in the Case 1 also in Case 2 the flow is supersonic in both the stator and rotor of the axial impulse turbine with a considerable degree of reaction. In the case of the radial-axial inflow turbine the flow is supersonic in the stator, but transonic in the rotor. Shockwaves structures are also similar to those described in Case 1.

The turbines which generate a relatively higher power (like these from Cases 2A and 2B, Tab. 3.1), usually do not cause the problems with the nozzle throat to the extent like that mentioned above because of the higher mass flow rate. For the same reason which is described in the chapter 3.1 the authors decide to choose the Case 2A as a target type of the turbine construction. Anyway in this case it has to be mentioned that the total generated power is much greater than it is in the Case 1, so the difference in the amount of isentropic efficiency between the cases: 2A and 2B is more important.

Table 11: The axial impulse turbine (with a considerable degree of reaction) main dimensions – Case 2A (MM fluid, 300 kW plant).

Control section	R [mm]	R_h [mm]	R_s [mm]	l [mm]	D/l [mm]	L_{ax} [mm]	b [mm]	Z [–]
Nozzle (outlet)	145.4	128.0	161.0	33.0	8.8	50.0	122.3	20/20
Rotor (outlet)	151.5	120.0	177.5	57.5	5.1	45.0	46.1	31

Table 12: The radial inflow reaction turbine main dimensions – Case 2B (MM fluid, 300 kW plant).

Control section	R [mm]	R_h [mm]	R_s [mm]	l [mm]	D/l [mm]	L_{ax} [mm]	b [mm]	Z [–]
Nozzle (outlet)	241.6	241.6	241.6	12.1	40.0	12.1	60.4	32/32
Rotor (outlet)	140.1	69.0	150.0	116.8	2.40	176.4	294.5	11

Table 13: Kinematics values of the mean stream – Case 2A (MM fluid, 300 kW plant).

Control section	c [m/s]	w [m/s]	u [m/s]	α [°]	β [°]	M [–]	Δh_s [kJ/kg]	u/c_s [–]
Nozzle (outlet)	324.25	118.98	220.84	12.62	36.55	2.168	7.14	0.57
Rotor I (outlet)	115.93	231.69	230.05	76.24	150.92	1.550	5.13	

Table 14: Performance of the axial impulse turbine (with a considerable degree of reaction) – Case 2B (MM fluid, 300 kW plant).

P_{NET} [kW]	η_{NET} [%]	$\eta_{\mathrm{NET\_CFD}}$ [%]	Θ_h [%]
365.50	76.9	80.9	8.0

Table 15: Kinematics values of the mean stream – Case 2B (MM fluid, 300 kW plant).

Control section	c [m/s]	w [m/s]	u [m/s]	α [°]	β [°]	M [–]	Δh_s [kJ/kg]	u/c_s [–]
Nozzle (outlet)	271.51	48.39	278.29	10	103.03	1.84	3.20	0.685
Rotor I (outlet)	63.65	173.59	161.41	90.08	158.49	1.17	2.87	0.675

Table 16: Performance of the radial inflow reaction turbine – Case 2B (MM fluid, 300 kW plant).

P_{NET} [kW]	η_{NET} [%]	$\eta_{\mathrm{NET\_CFD}}$ [%]
428.61	90.2	88.99

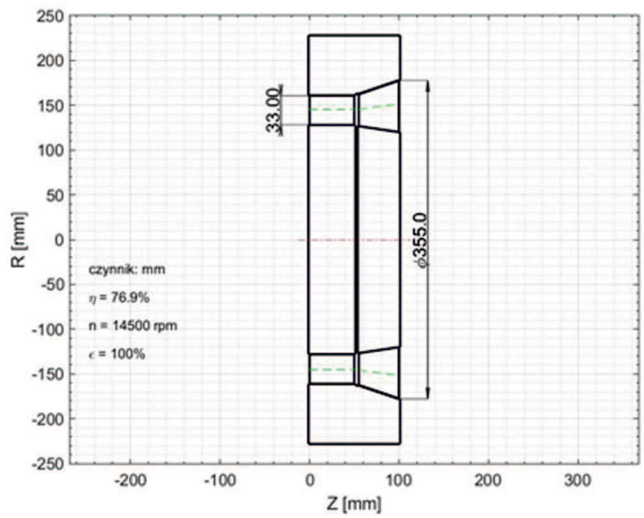

Figure 10: The axial impulse turbine (with considerable degree of reaction) stage sketch – Case 2A (MM fluid, 300 kW plant).

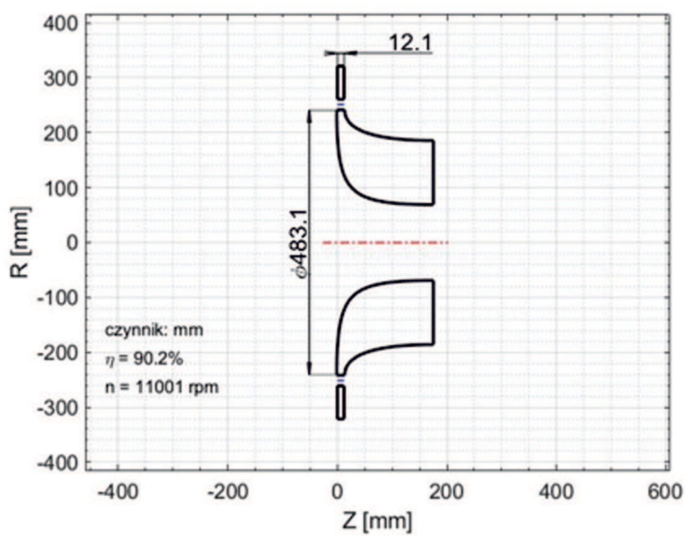

Figure 11: The radial inflow reaction turbine main dimensions – Case 2B (MM fluid, 300 kW plant).

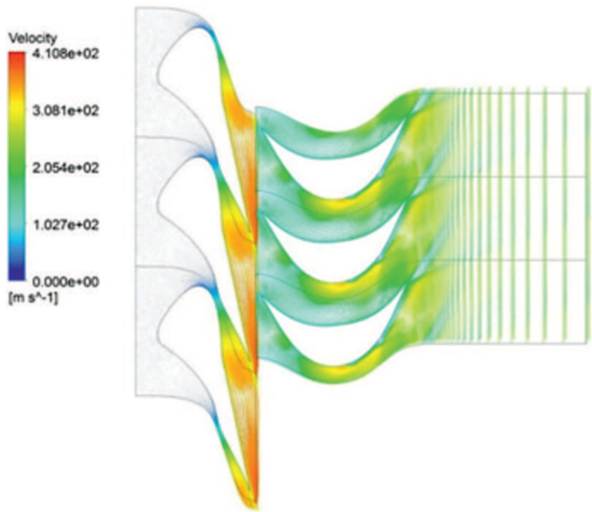

Figure 12: Velocity vectors at the mean diameter of the axial impulse turbine (with considerable degree of reaction) – Case 2A (MM fluid, 300 kW plant).

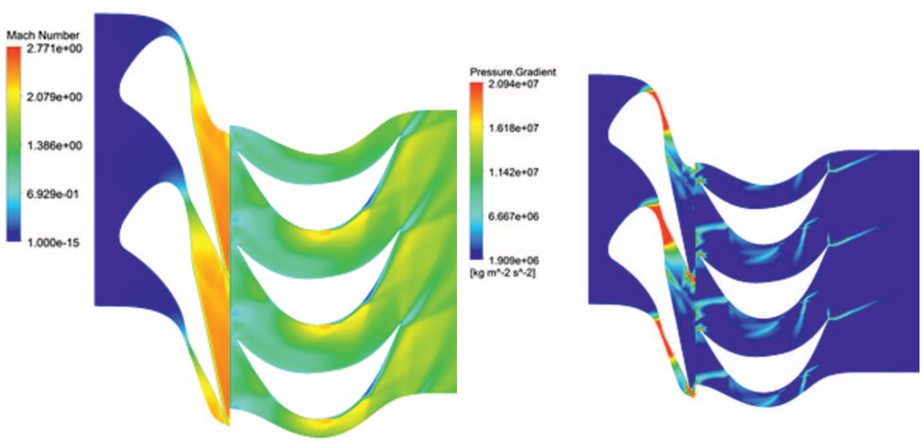

Figure 13: Mach Number contours (left side) and pressure gradient contours (right side) at the mean diameter of the axial impulse turbine (with considerable degree of reaction) – Case 2A (MM fluid, 300 kW plant).

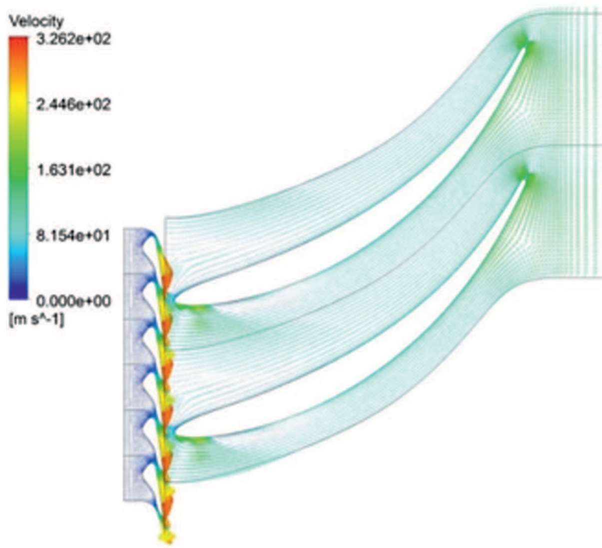

Figure 14: Velocity vectors at the mean diameter of the radial reaction turbine – Case 2B (MM fluid, 300 kW plant).

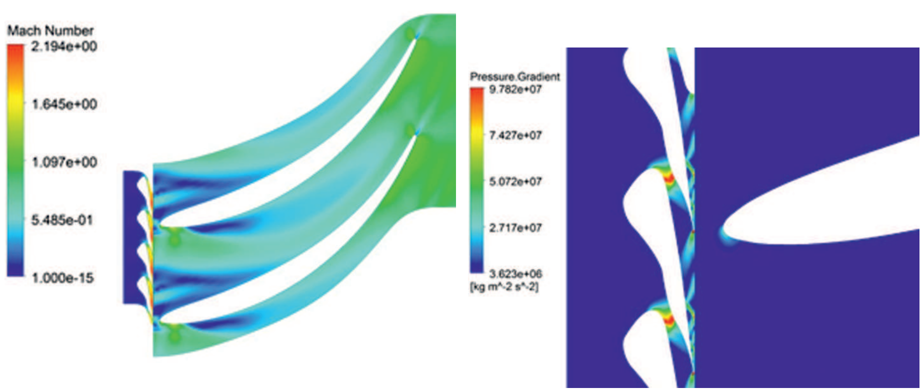

Figure 15: Mach Number contours (left side) and pressure gradient contours (right side) at the mean diameter of the radial reaction turbine – Case 2B (MM fluid, 300 kW plant).

4 Summary

A number of ORC turbine designs including impulse-type and radial-type turbines have been analysed in the paper from the point of view of flow efficiency, mechanical and machining aspects. It follows from the analysis of results presented in the paper that for ORC power plants, especially micro power plants, the suitable choice of a turbine is the axial impulse turbine with a considerable degree of reaction (about 25% at the mean radius). It is a compromise between small dimensions, acceptable axial thrust, relatively high efficiency and simplicity of machining. This compromise provides that this type of turbine can be recommended to use as a part of a compact and hermetic micro turbogenerator for ORC power plant whose main goal is usually to generate the maximum possible power not necessarily with the highest efficiency.

Acknowledgements This work has been partially founded by by The National Centre for Research and Development and by The Smart Growth Operational Programme (European funds) within the project No. POIR.01. 01.01-00-0414/17 and POIR.01.01.01-00-0512/16 carried out jointly with the Marani Company. Calculations were carried out at the Academic Computer Centre in Gdańsk.

Received 12 December 2018

References

[1] Perycz S.: *Steam and Gas Turbines.* Ossolineum, Wrocław Warszawa Kraków 1992 (in Polish).

[2] Japikse D., Baines N.C.: *Introduction to Turbomachinery.* Concepts ETI, 1994.

[3] Dixon S.L.: *Fluid Mechanics and Themodynamics of Turbomachinery* (5th Edn.). Pergamon Press, 2005.

[4] Fiaschi D., Manfrida G., Maraschiello F.: *Thermo-fluid dynamics preliminary design of turbo-expanders for ORC cycles. Appl. Energ.*. **97**(2012), 601–608.

[5] Pini M., Perisco G., Casati E., Dossena V.: *Preliminary design of a centrifugal turbine for ORC applications.* In: Proc. 1st Int. Sem. on ORC Power Systems ORC 2011, Delft 2011.

[6] Spadacini C., Rizzi D., Saccilotto C., Salgorollo S., Centemeri L.: *The radial outflow turbine technology.* In: Proc. 2nd Int. Sem. on ORC Power Systems ASME ORC 2013, Rotterdam 2013.

[7] Harinck J., Pasquale D., Pecnik R., van Buijtenen J., Colonna L.: *Performance improvement of a radial organic Rankine cycle turbine by means of automated computational fluid dynamic design*. Proc. Inst. Mech. Eng. A J. Power Energy **227**(2013), 637–645.

[8] Klonowicz P., Bröggemann D.: *2D unsteady RANS simulations of an organic vapor partial admission turbine*. In: Proc. 2nd Int. Sem. on ORC Power Systems ASME ORC 2013, Rotterdam 2013.

[9] Kiciński J., Żywica G.: *Steam Microturbines in Distributed Cogeneration*. Springer International Publishing, 2014.

[10] Weiss A.P., Popp T., Müller J., Brüggemann , Preissinger M.: *Experimental characterization and comparison of an axial and a cantilever micro-turbine for small-scale Organic Rankine Cycle*, *Appl. Therm. Eng.* **140**(2018), 235–244.

[11] Weiss A.P.: *Volumetric expanders versus turbine – which is the better choice for small ORC plants?* In: Proc. 3rd Int. Sem. on ORC Power Systems, Brussels 2015.

[12] Klonowicz P., Hanausek P.: *Optimum design of the axial ORC turbines with support of the Ansys CFX flow*. In: Proc. 1st Int. Sem. on ORC Power Systems ORC 2011, Delft 2011.

[13] Ansys Academic Research CFX, Release 19.1.

[14] Klonowicz P., Heberle F., Preissinger M., Brüggemann D.: *Significance of loss correaltions in performance prediction of small scale, highly loaded turbine stages working in Organic Rankine Cycles*. *Energy* **72**(2014), 322–330.

[15] Traupel W.: *Thermische Turbomaschinen*. Springer Singapore Pte., 2001.

[16] Ansys Academic BladeGen, Release 19.1.

[17] Kosowski K., Piwowarski M., Stępień R., Włodarski W.: *Design and investigations of the ethanol microturbine.* Arch. Thermodyn. **39**(2018), 2, 41–54.

[18] Wajs J., Mikielewicz D., Bajor M., Kneba Z.: *Experimental investigation of domestic micro-CHP based on the gas boiler fitted with ORC module*. Arch. Thermodyn. **37**(2016), 3, 79–93.